Impact of Secondary Eyewall Heating on Tropical Cyclone Intensity Change*

XIAQIONG ZHOU, BIN WANG, XUYANG GE, AND TIM LI

International Pacific Research Center, and Department of Meteorology, School of Ocean and Earth Science and Technology, University of Hawaii at Manoa, Honolulu, Hawaii

(Manuscript received 3 August 2010, in final form 22 October 2010)

ABSTRACT

The primary goal of this study is to explore the factors that might influence the intensity change of tropical cyclones (TCs) associated with secondary eyewall replacement. Concentric eyewall structures in TCs with and without large intensity weakening are compared using the Tropical Rainfall Measuring Mission (TRMM) 2A12 and 2A25 data. It is found that the secondary eyewalls with a stratiform-type heating profile show a marked weakening, while those TCs with a convective-type heating weaken insignificantly or even intensify. This observed feature is supported by a set of sensitivity numerical experiments performed with the Weather Research and Forecasting model. With more active convection, the latent heat released in the outer eyewall and moat region can better sustain storm intensity. The prevailing stratiform precipitation results in low equivalent potential temperature air in the moat and reduces the entropy of the boundary layer inflow to the inner eyewall through persistent downdrafts, leading to a large intensity fluctuation. Comparison of observations and numerical model results reveals that the model tends to overproduce convective precipitation in the outer eyewall and the moat. It is possible that the model underestimates the storm intensity changes associated with eyewall replacement events.

1. Introduction

Concentric eyewalls usually refer to two or more quasi-circular eyewalls separated by a convective minimum region, known as a moat, in intense tropical cyclones (TCs) (Fortner 1956; Willoughby et al. 1982; Black and Willoughby 1992; Hawkins et al. 2006). As the outer eyewall forms, the inner one weakens and is eventually replaced by the outer one. Large intensity fluctuations are usually expected. However, observations show that intensity changes associated with eyewall replacement can vary greatly with cases. For example, an abrupt decrease in the maximum wind speed as large as 46 m s^{-1} was detected in Typhoon Sarah (1956), but the appearance of the concentric eyewalls in Hurricane Anita (1977) only marks the end of a deepening phase (Fortner 1956; Willoughby et al. 1982). Kuo et al. (2009) examined the intensity changes before and after concentric eyewall formation over the western North Pacific (WNP). The storms that intensify before the secondary eyewall formation but weaken afterward account for about 49% of all cases. In about 22% of cases, the formation of secondary eyewalls only slows down the intensification rate. In about 4% of the concentric eyewall cases, the weakening storms even gain intensity after the secondary eyewall formation. The diversity of the intensity changes in TCs with secondary eyewalls suggests that accurate intensity forecasts are not guaranteed even if we can predict the formation of secondary eyewalls.

Our ability to observe concentric eyewalls has been greatly improved through in situ means and by remote sensing. The passive microwave remote sensing can penetrate the upper-level cloud shield and allow us to view the storm convective structures with more clarity. Concentric eyewall events can be successfully identified by utilizing passive microwave products for global tropical cyclone monitoring (Hawkins et al. 2006; Kossin and Sitkowski 2009; Kuo et al. 2009). However, the detailed structures of concentric eyewalls have not been examined.

The primary goals of this study are (a) to investigate whether the thermodynamic structures differ between the concentric eyewall TCs with and without large intensity

* School of Ocean and Earth Science and Technology Contribution Number 8040 and International Pacific Research Center Contribution Number 735.

Corresponding author address: Xiaqiong Zhou, University of Hawaii, 2525 Correa Rd., HIG 351A, Honolulu, HI 96822.
E-mail: xiaqiong@hawaii.edu

DOI: 10.1175/2010JAS3624.1

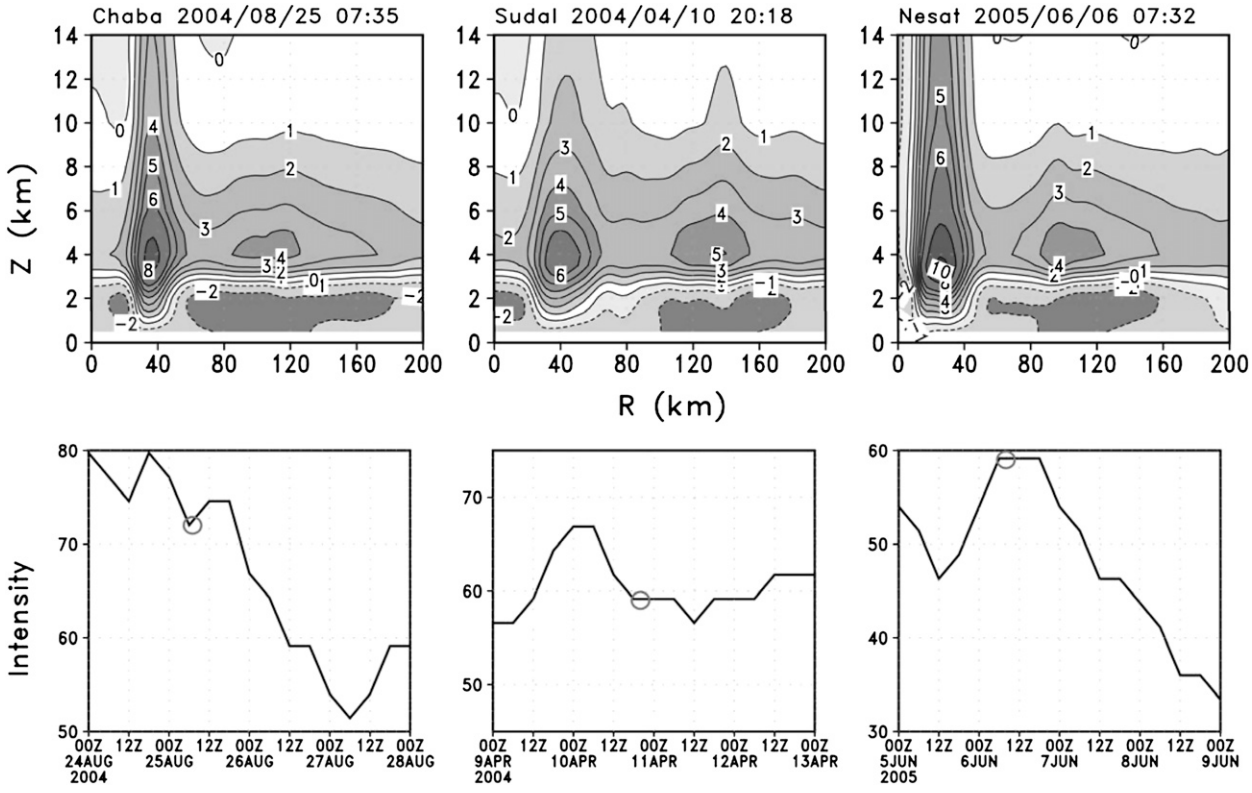

FIG. 1. (top) The symmetric component of diabatic heating rates (K h^{-1}) according to the TRMM 2A12 dataset and (bottom) the time evolution of TC intensity (m s^{-1}) for LC TCs. The time of TRMM 2A12 snapshots is indicated by an open circle in the bottom panels.

fluctuation and (b) to investigate whether the secondary eyewalls and associated intensity fluctuation simulated by numerical models are consistent with the observations.

2. Data and methodology

The Tropical Rainfall Measuring Mission (TRMM) 2A12 dataset (Olson et al. 2006) is generated from TRMM Microwave Imager (TMI) brightness temperatures by blending the radiometric data with dynamical cloud models. The swath width of the TRMM 2A12 is 878 km. The dataset has 5.1-km horizontal resolution and 14 vertical layers from the surface to 18.0 km. The TRMM 2A25 (Iguchi et al. 2000) provides three-dimensional rain rate and radar reflectivity measured by the TRMM Precipitation Radar (PR) with 247-km swath width and 5-km horizontal resolution. The limited spatial and temporal coverage cannot describe the entire cycle of eyewall replacement, but it provides some snapshots of TCs with concentric eyewall structure.

The cases with quasi-circular secondary eyewalls captured by TRMM orbits are selected. To avoid the influence of the cold underlying ocean surface or frictional boundary on storm intensity, storms moving north of 25°N or close to land are discarded. As a result, only a few cases are available.

The track and intensity of each storm come from the best-track database of the Joint Typhoon Warning Center (JTWC). Two sample groups of TCs are classified based on the intensity fluctuation. In the first group, the typhoons, including Typhoons Chaba (2004), Sudal (2004), and Nesat (2005), exhibit a large fluctuation in the maximum surface wind velocity (>10 m s^{-1}) when concentric eyewalls are identified (Fig. 1). This group is labeled as the ''large change'' group (LC). In the second group, called the ''small change'' group (SC), the storms, including Typhoons Pudal (2001), Dujuan (2003), and Lupit (2003), experience a small intensity fluctuation or even an increase (Fig. 2).

3. Observations

Although the retrieval of latent heating from the TRMM measurements is still undergoing development and improvement, the general structure of latent heating for a tropical cyclone can be reasonably presented (Tao et al. 2006). The azimuthally averaged component of diabatic heating shows that there are two heating maxima

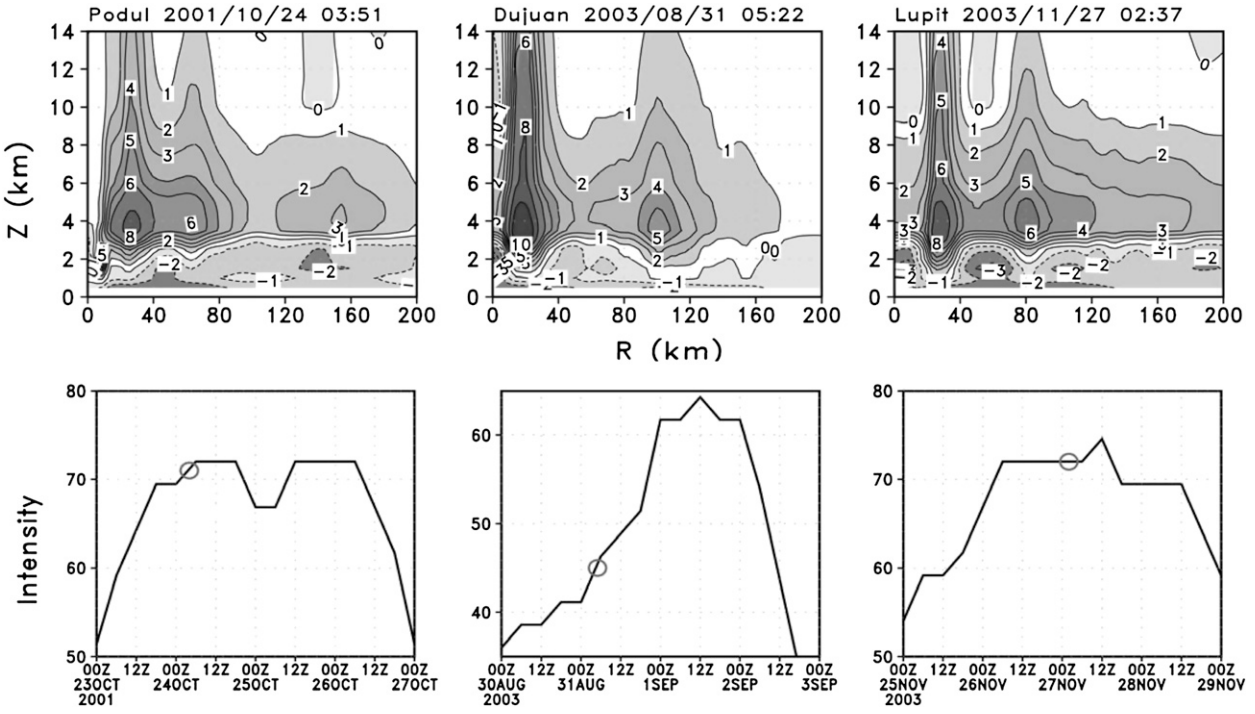

FIG. 2. As in Fig. 1, but for SC TCs.

associated with each of the concentric eyewalls (Figs. 1 and 2). The inner eyewalls are expected to decay after the formation of the secondary eyewalls. Since they remain much stronger and extend deeper into the free atmosphere than the outer ones in these six snapshots, it suggests that the storms observed are at the early stage of the eyewall replacement. In LC, the heating (cooling) occurs above (below) a height of 3 km in the moat and outer eyewall region. The upper-level heating shows a flat top below 10 km in the outer eyewall. Generally, the low-level diabatic cooling is a result of the evaporation of rain droplets or snow melting below the freezing level. The heating profile suggests that stratiform-type precipitation prevails in the outer region. Meanwhile, the storm weakens rapidly when concentric eyewalls are identified. A weak reintensification following the rapid decay in Typhoons Chaba (2004) and Sudal (2004) is a result of the contraction and the organization of the outer eyewalls (not shown).

In contrast, strong convective heating of the outer eyewalls in SC penetrates upward beyond 14 km, which is much deeper than those in LC. Meanwhile, the cooling rate below the freezing level is much weaker. The results suggest that convective precipitation dominates in the outer region. Notice that there is no significant intensity change in Typhoons Podul (2001) and Lupit (2003), and Typhoon Dujuan (2003) even intensifies after the secondary eyewall forms.

TRMM 2A25 provides more accurate data since it directly measures the intensity of convection. However, its swath width is much narrower than that of 2A12, so only four of six TCs of interest are captured. In this study, maximum radar reflectivity in the vertical that exceeds 40 dBZ is considered deep convection. The coverage of deep convection reaches the peak in concentric eyewalls (Fig. 3). The proportion of deep convection in the outer eyewalls is below 35% in LC, whereas it reaches 60% in SC.

The observations suggest that intensity change associated with secondary eyewall replacement is related to the thermodynamic features of the outer eyewall and the moat. Active deep convection in the outer eyewall and the moat region likely leads to a small intensity fluctuation or even an increase during the eyewall replacement, whereas more stratiform-like precipitation prevailing in these areas is responsible for a large intensity fluctuation. Admittedly, the number of samples is too small to conduct a statistical test. Therefore, we conduct a set of numerical sensitivity experiments to confirm the TRMM findings.

4. Sensitivity experiments

It is generally accepted that broad-scale downdrafts indicative of stratiform rain are initiated and maintained

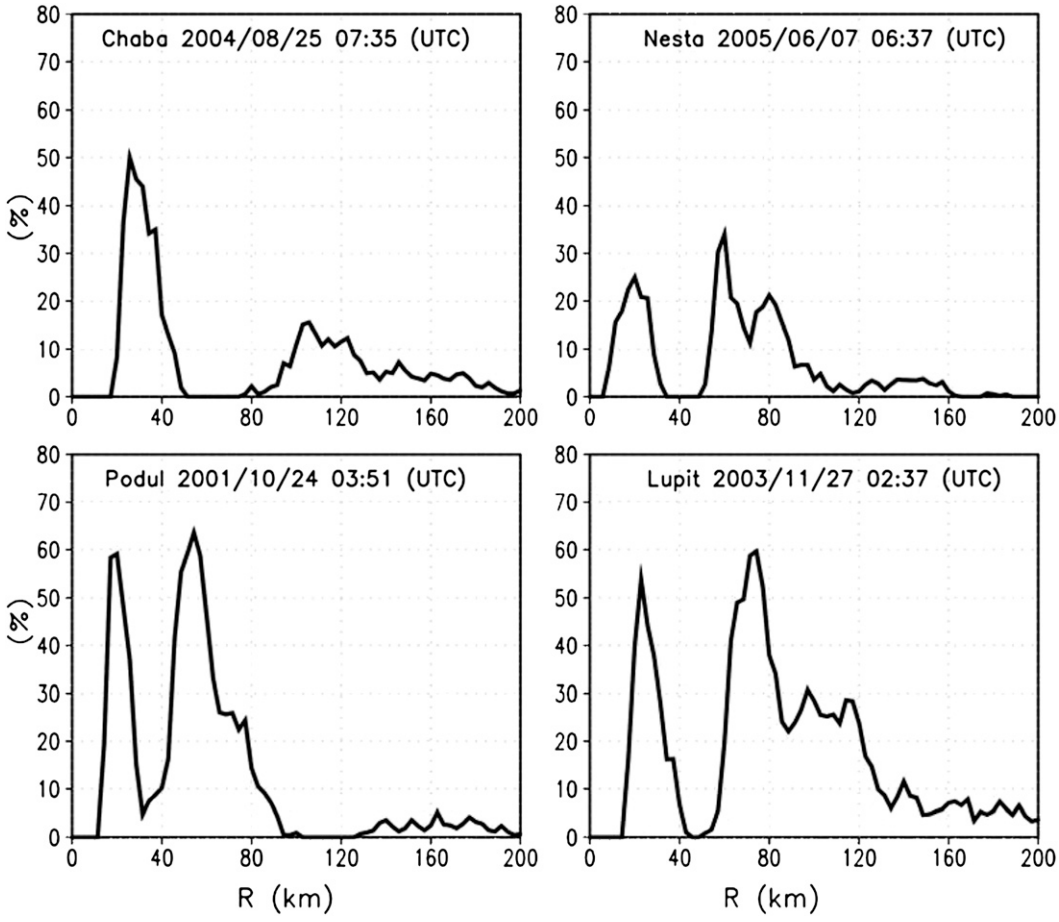

FIG. 3. The radial distributions of the deep convection coverage (maximum radar reflectivity > 40 dBZ) in (top) LC and (bottom) SC.

by light ice particles (Lord et al. 1984; Willoughby et al. 1984; Tao and Simpson 1989). To change the proportion of deep convection and stratiform clouds, two sensitivity numerical experiments were conducted using the Weather Research and Forecasting (WRF) model. The model is conducted in a quadruply nested two-way interactive mode with the horizontal resolutions of 54, 18, 6, and 2 km, respectively, and 28 levels in the vertical. The vortex is embedded on an f plane centered at 18°N in a quiescent environment over the ocean with a constant sea surface temperature of 29°C. A detailed description of the control experiment can be found in Zhou and Wang (2009). The sensitivity run (hereafter ICE) makes use of identical initial conditions and model parameters as the control run (CTL), except that concentrations of ice particles in the microphysics package (Lin et al. 1983) are enhanced. The formation of a secondary eyewall and eyewall replacement are well simulated in both experiments. The full cycles of the secondary eyewall replacement in these two experiments are compared in Zhou and Wang (2011). Here, only the thermodynamic features of concentric eyewalls and associated intensity fluctuation are examined to compare with the observations (Figs. 4 and 5).

The modification of the ice-phase microphysics significantly affects concentric eyewall structures. The outer eyewall in CTL is located closer to the inner one than in ICE, and the cooling in the moat is weaker (Fig. 4). The heating rate of the secondary eyewall in CTL is larger than in ICE, although the coverage of deep convection in the outer eyewalls is basically similar (Fig. 5). Overall, convection outside of the inner eyewall is more active in CTL than in ICE. Suppressed convection in ICE is ascribed to the enhanced concentrations of snow and cloud ice at the upper-tropospheric outflow layer. The storm in ICE has a more distinct subsidence region (moat) surrounding the inner eyewall than that in CTL due to the reinforced cooling of ice particles melting as they fall into the warm air. Note that the maximum surface wind speed decreases more than 10 m s^{-1} in ICE and only about

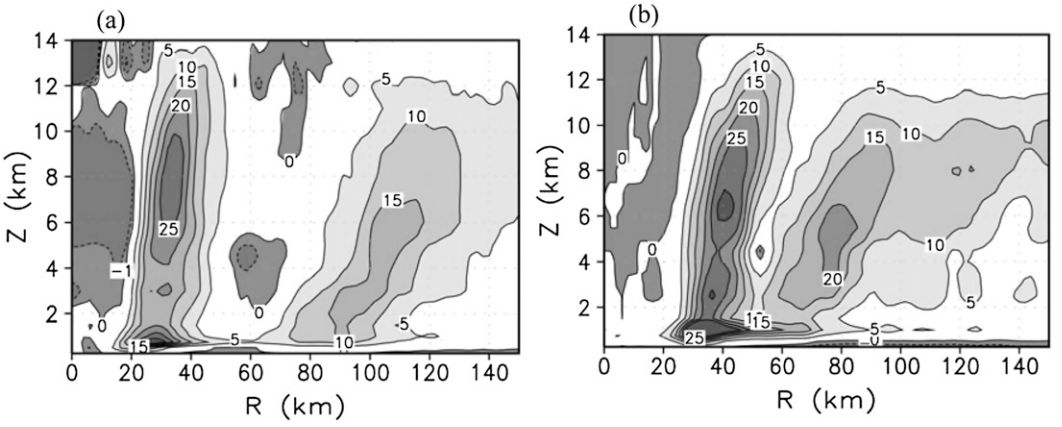

FIG. 4. The symmetric component of diabatic heating rates (K h^{-1}) averaged in the first 3 h after the formation of the secondary eyewall in the (a) ICE and (b) CTL experiments simulated by the WRF model.

5 m s^{-1} in CTL (Fig. 5). Apparently, the sensitivity experiment result is consistent with the observations.

The simulated outer eyewall tilts outward with altitude, while it is upright in the TRMM data (Figs. 1 and 2). This is likely due to the relatively coarse horizontal resolution (about 5 km) compared with the model (2 km). It is worth noting that the simulated heating rate in concentric eyewalls is generally greater than in the observed cases. The simulated low-level cooling associated with snow melting and evaporation is also much weaker and shallower. The percentage of deep convection further indicates that the model storm is too convective in the eyewalls and moat regions (Fig. 5). The coverage of deep convection in the outer eyewalls in the model (>80%) is

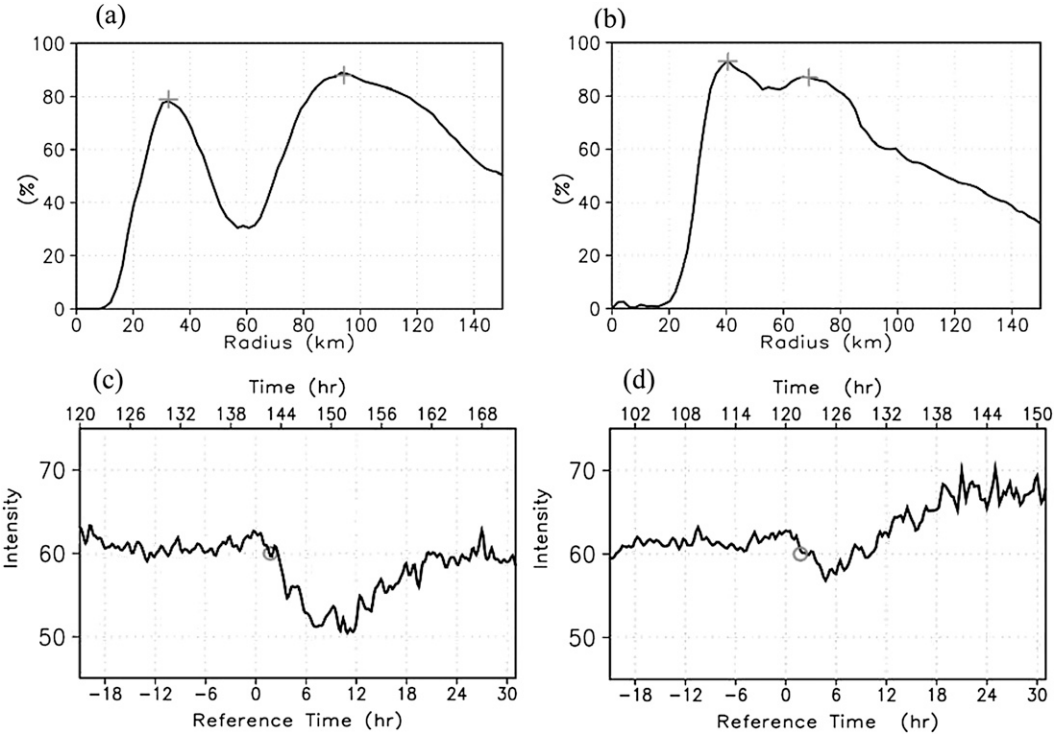

FIG. 5. (a),(b) Radial distributions of the deep convection coverage (the maximum radar reflectivity > 40 dB*Z*) in (a) ICE and (b) CTL. (c),(d) Time series of storm intensity (m s^{-1}) for (c) ICE and (d) CTL. The open circles mark the time for (a) and (b). The time of the model integration and the reference time with respect to the secondary eyewall formation are indicated at the upper and lower *x* coordinates.

much greater than in the observed cases (<60%). The moat is almost free of deep convection (Fig. 3) in the TRMM measurements, whereas the coverage of deep convection in the moat is high in the model (Fig. 5). The enhanced concentrations of ice particles in ICE lead to a clear moat and suppressed convection in the outer region but do not qualitatively change the heating profile. Unrealistically strong convection simulated by the model would result in underestimated storm intensity fluctuations.

5. Interpretation

The diabatic heating in the outer region has a direct effect on the storm intensity during eyewall replacement. As the inner eyewall dies, the storm temporarily loses its ability to produce an intense, localized warm core so the storm weakens (Rozoff et al. 2008). The new eyewall must have the ability to maintain a warm core not only in the previous eye but also in the moat region to prevent the weakening of the storm. The ability of a new eyewall with prevailing deep convection (stratiform clouds) to maintain the storm intensity would be high (weak). Meanwhile, the moat becomes a part of the eye after the inner eyewall fades away. If the stratiform-type precipitation prevails in the moat, the air in the moat is characterized by low equilibrium potential temperature θ_e at the middle levels. To recover the intensity, the low θ_e in the moat must be filled. The prevailing stratiform-type precipitation in the moat would lead to large intensity fluctuation during eyewall replacement.

In addition to the direct influence, the storm intensity change would be affected by the heating-induced secondary circulation. The response of secondary circulations to convective- and stratiform-type heating in an intense storm is confirmed by Moon and Nolan (2010) using a three-dimensional, nonhydrostatic, linear model of the vortex-anelastic equations. In the region where stratiform-type clouds prevail, weak downdrafts and evaporation cooling dominate below the environmental 0°C level, and weak updrafts and diabatic heating appear in the middle to upper levels. In convective regions, strong updrafts and diabatic heating dominate through the troposphere (Shapiro and Willoughby 1982). If stratiform-type precipitation prevails in the outer eyewall and moat, persistent downdrafts from the lower and middle troposphere into the boundary layer may reduce the boundary layer θ_e. From the perspective of an idealized Carnot-cycle heat engine (Emanuel 1986), when lower θ_e airs enter the core region of the TC, a decrease of storm intensity can be expected (Barnes et al. 1983). In other words, the appearance of stratiform (convective)-type heating profiles in the outer region would lead to a large (small) fluctuation of storm intensity during eyewall replacement. Since the numerical model generates less (more) stratiform (convective)-type precipitation, this indirect process would play a minor role in weakening storm intensity. In this regard, the intensity fluctuation during eyewall replacement cycles might be underestimated by the model.

6. Summary

The vertical thermodynamic structures of concentric eyewalls in those TCs with and without significant intensity fluctuation are compared by using TRMM 2A12 and 2A25 satellite data. The observed features are further examined through a set of numerical simulations by using the Weather Research and Forecasting (WRF) model. The model can realistically simulate secondary eyewall replacement cycles and associated intensity changes. Both the observation and model results suggest that the weakening of a TC is more (less) significant when stratiform-type (convective-type) precipitation prevails in the secondary eyewall and the moat. The latent heating released in a new eyewall with more active convection can better maintain the storm intensity, whereas prevailing stratiform precipitation in the moat and outer eyewall will reduce the boundary layer inflow θ_e to the inner eyewall through persistent downdrafts and result in low-θ_e air in the moat. These two possible ways to generate low-θ_e air in the inner core region could lead to a large intensity fluctuation during the eyewall replacement. On the other hand, the model tends to overproduce deep convection, suggesting that the model possibly underestimates the weakening of storm intensity associated with secondary eyewall replacement cycles.

Acknowledgments. This research was supported by Dr. Ramesh Kakar through NASA project NNX09AG97G. It is also supported by ONR Grant N000141010774.

REFERENCES

Barnes, G. M., E. J. Zipser, D. P. Jorgensen, and F. D. Marks Jr., 1983: Mesoscale and convective structure of a hurricane rainband. *J. Atmos. Sci.,* **40,** 2125–2137.

Black, M. L., and H. E. Willoughby, 1992: The concentric eyewall cycle of Hurricane Gilbert. *Mon. Wea. Rev.,* **120,** 947–957.

Emanuel, K. A., 1986: An air–sea interaction theory for tropical cyclones. Part I: Steady-state maintenance. *J. Atmos. Sci.,* **43,** 585–605.

Fortner, L. E., 1956: Typhoon Sarah. *Bull. Amer. Meteor. Soc.,* **39,** 633–639.

Hawkins, J. D., M. Helveston, T. F. Lee, F. J. Turk, K. Richardson, C. Sampson, J. Kent, and R. Wade, 2006: Tropical cyclone multiple eyewall configurations. *Extended Abstracts, 27th*

Conf. on Hurricanes and Tropical Meteorology, Monterey, CA, Amer. Meteror. Soc., 6B.1. [Available online at http://ams.confex.com/ams/27Hurricanes/techprogram/paper_108864.htm.]

Iguchi, T., T. Kozu, R. Meneghine, J. Awaka, and K. Okamoto, 2000: Rain-profiling algorithm for the TRMM precipitation radar. *J. Appl. Meteor.,* **39,** 2038–2052.

Kossin, J. P., and M. Sitkowski, 2009: An objective model for identifying secondary eyewall formation in hurricanes. *Mon. Wea. Rev.,* **137,** 876–892.

Kuo, H.-C., C.-P. Chang, Y.-T. Yang, and H.-J. Jiang, 2009: Western North Pacific typhoons with concentric eyewalls. *Mon. Wea. Rev.,* **137,** 3758–3770.

Lin, Y.-L., R. D. Farley, and H. D. Orville, 1983: Bulk parameterization of the snow field in a cloud model. *J. Climate Appl. Meteor.,* **22,** 1065–1092.

Lord, S. J., H. E. Willoughby, and J. M. Piotrowicz, 1984: Role of a parameterized ice-phase microphysics in an axisymmetric tropical cyclone model. *J. Atmos. Sci.,* **41,** 2836–2848.

Moon, Y., and D. S. Nolan, 2010: The dynamic response of the hurricane wind field to spiral rainband heating. *J. Atmos. Sci.,* **67,** 1779–1805.

Olson, W. S., and Coauthors, 2006: Precipitation and latent heating distributions from satellite passive microwave radiometry. Part I: Improved method and uncertainties. *J. Appl. Meteor. Climatol.,* **45,** 702–720.

Rozoff, C. M., W. H. Schubert, and J. P. Kossin, 2008: Some dynamical aspects of tropical cyclone concentric eyewalls. *Quart. J. Roy. Meteor. Soc.,* **134,** 583–593.

Shapiro, L. J., and H. E. Willoughby, 1982: The response of balanced hurricanes to local sources of heat and momentum. *J. Atmos. Sci.,* **39,** 378–394.

Tao, W.-K., and J. Simpson, 1989: Modeling study of a tropical squall-type convective line. *J. Atmos. Sci.,* **46,** 177–202.

——, and Coauthors, 2006: Retrieval of latent heating from TRMM measurements. *Bull. Amer. Meteor. Soc.,* **87,** 1555–1572.

Willoughby, H. E., J. A. Clos, and M. G. Shoreibah, 1982: Concentric eye walls, secondary wind maxima, and the evolution of the hurricane vortex. *J. Atmos. Sci.,* **39,** 395–411.

——, H.-L. Jin, S. J. Lord, and J. M. Piotrowicz, 1984: Hurricane structure and evolution as simulated by an axisymmetric, nonhydrostatic numerical model. *J. Atmos. Sci.,* **41,** 1169–1186.

Zhou, X., and B. Wang, 2009: From concentric eyewall to annular hurricane: A numerical study with the cloud-resolved WRF model. *Geophys. Res. Lett.,* **36,** L03802, doi:10.1029/2008GL036854.

——, and ——, 2011: Mechanism of concentric eyewall replacement cycle and associated intensity change. *J. Atmos. Sci.,* in press.